Current **A**pplied **S**cience and **T**echnology e-ISSN: 2586-9396

Curr. Appl. Sci. Technol. 2027, Vol. 27 (No. 1), e0269565

Research article

Isolation of a Metal-Tolerant *Serratia marcescens* for Cu(II) and Pb(II) Biosorption: Elucidating Transport and Attachment Mechanisms

Clint Sutherland[1]* and Vasyl Karabyn[2]

[1]Project Management and Civil Infrastructure Systems, University of Trinidad and Tobago, Trinidad, W.I.
[2]Department of Civil Protection, Lviv State University of Life Safety, Lviv, Ukraine

Received: 19 October 2025, Revised: 13 January 2026, Accepted: 30 January 2026, Published: 10 April 2026

Abstract

This study explores the biosorptive potential of a metal-tolerant strain of *Serratia marcescens* isolated from soil near an underground fuel storage tank, for the removal of Cu(II) and Pb(II) from aqueous solutions. Batch biosorption experiments were conducted to assess kinetic and equilibrium behaviour. The Weber and Morris intraparticle diffusion and the diffusion-chemisorption (D-C) models were applied to elucidate transport mechanisms. Langmuir and the Freundlich isotherms were used for equilibrium modelling. Individual and sequential desorption tests using distilled water, $CaCl_2$, EDTA and HCl were performed to identify the nature of attachment mechanisms. Both metals reached equilibrium within 60 min, with Cu(II) showing a faster uptake rate (half-time 2.2 min) than Pb(II) (13.9 min). Surface adsorption and intracellular diffusion were identified as the dominant transport pathways, with the D-C model indicating a stronger diffusion contribution for Pb(II) (R_{DC} = 0.392) than for Cu(II) (R_{DC} = 0.156). Langmuir analysis yielded monolayer capacities of 34.4 mg/g for Cu(II) and 22.2 mg/g for Pb(II). Desorption studies using distilled water, $CaCl_2$, EDTA and HCl provided insight into binding mechanisms. $CaCl_2$ and EDTA each desorbed 47.3% of Cu(II), suggesting a notable influence by ion-exchange and complexation, while HCl released 4.5%, consistent with intracellular accumulation. This study highlights the multifaceted biosorption of Cu(II) and Pb(II) by *S. marcescens*. Integrating kinetic, equilibrium and desorption analyses provide mechanistic clarity, which guides optimization and regeneration strategies and strengthens the biosorbent's practical value for cost-effective, sustainable heavy metal remediation.

Keywords: *Serratia marcescens;* biosorption; desorption; mechanisms; kinetic modelling; heavy metals

*Corresponding author: E-mail: clint.sutherland@utt.edu.tt
https://doi.org/10.55003/cast.2026.269565
Copyright © 2026 by King Mongkut's Institute of Technology Ladkrabang, Thailand. This is an open access article under the CC BY-NC-ND license (http://creativecommons.org/licenses/by-nc-nd/4.0/).

1. Introduction

The remediation of heavy metals from industrial discharges continues to be a major financial burden, particularly for small- and medium-sized industries (Ashraf et al., 2024). Despite increased awareness of the adverse impacts of heavy metals, numerous studies continue to report the widespread occurrence of heavy metals in the environment at concentrations exceeding regulatory limits (Sutherland et al., 2017; Karabyn & Kochmar, 2025). For example, Fardullah et al. (2025) reported concentrations of chromium, lead and nickel of 0.66, 0.16 and 1.9 mg/L, respectively, in water at Tanguar Haor in Bangladesh. In sediments of the Great Bačka Canal in Serbia, Pejin et al. (2025) detected copper, nickel and zinc at concentrations of 155, 46.5 and 344.8 mg/kg, respectively. Similarly, groundwater samples from the Shazand Plain in Iran exhibited chromium and zinc concentrations of 19.0 and 22.8 µg/L, respectively (Sharafi & Salehi, 2025). Kochmar et al. (2022) reported that, across coal-mine spoil lithologies at the Vizeyska site (Ukraine), total Pb ranged from 4.72 to 16.97 mg/kg; ammonium acetate–extractable (bioavailable) and water-extractable Pb constituted 7-21% and 3-15% of the total, respectively. Metal migration increases significantly in the event of spontaneous combustion of coal dumps, which occurs in the region. At the national scale, Ukraine hosts over 1,300 coal-mine waste heaps, forming a widespread and long-lived source of metal release**.** In the district, well water has intermittently met or exceeded the maximum allowable concentration for Pb, with implications for civil protection and emergency risk management (Kochmar et al., 2024). The composition and concentration of heavy metals in industrial effluents vary markedly depending on the type of industry. For instance, Meshram et al. (2020) reported a lead concentration of 11.2 mg/L in effluent from a battery recycling facility in Chhattisgarh, India. In contrast, Mella et al. (2015) recorded a total chromium concentration of 2000.0 mg/L in tannery wastewater from Brazil.

Acute environmental incidents, such as the Minamata incident (Fuge, 2012) and the Baia Mare cyanide spill (Cunningham, 2005) have been caused by human activities. In addition, chronic environmental and occupational exposure can also lead to progressive health effects because many heavy metals are bioaccumulative. In a recent study by Xing et al. (2017), the levels of cadmium and lead in rice crops, as well as in blood and hair samples from farmers residing near mining areas in China were investigated. The study found a positive correlation between the concentration of cadmium in rice (0.06 mg/kg) and cadmium in human blood (8.0 µg/L). Similarly, a strong positive correlation was also observed between lead concentrations in soil and lead levels in human hair and blood, suggesting a direct environment-to-human transfer pathway. Another major source of human exposure is workplace-related or occupational exposure. Field assessments also flag potential hazards in sedimentary matrices (Al-Bahathy et al., 2024; Loboichenko et al., 2024). Othman and Hussein (2025) conducted a notable study of heavy metal concentrations in workers at a concrete block factory in Sulaymaniyah, Iraq. The authors reported mean concentrations of chromium, lead, cadmium, nickel and copper in male workers of 13.2, 25.7, 16.2, 8.6 and 21.0 mg/L, respectively. Interestingly, the study also found a positive association between years of employment and the accumulation of heavy metals. This further underscores the risk associated with long-term occupational exposure.

The health effects of heavy-metal exposure are dose-dependent and vary by metal ion. Cadmium is linked to renal and pulmonary damage (Mahurpawar, 2015). Lead exposure causes neurological impairment and damage to the brain, nervous system and kidneys (Martin & Griswold, 2009). Arsenic can trigger cardiovascular and hepatic damage (Mudgal et al., 2010), while nickel is associated with lung and kidney damage (Bharti &

Sharma, 2022). Hexavalent chromium has been connected to neurological problems (Jomova et al., 2025). Copper is essential in trace amounts but, in excess, can cause oxidative cell damage and neurodegenerative disorders (Zahra et al., 2017). While only a brief overview of the health impacts is provided here, a more comprehensive assessment of heavy metal toxicity in humans and animals can be found in the works of Mitra et al. (2022) and Jomova et al. (2025).

Over the past decades, growing global concern over the environmental and health impacts of heavy metals has spurred extensive research into more efficient and cost-effective treatment technologies (Oladimeji et al., 2024). Conventional methods, such as electrocoagulation, chemical precipitation, ion exchange and reverse osmosis have all shown great promise for industrial applications. However, these technologies are not without shortfalls. Particularly due to the high energy requirements, the production of secondary sludge, difficulty achieving low residual concentrations and elevated operational cost (Chakraborty et al., 2022; Sutherland, 2024). Adsorption has often emerged as a cost-effective method for contaminant removal. However, the cost of adsorbents varies significantly by region, influenced by factors such as the availability of raw materials, local expertise, and energy prices. The use of bacteria for heavy metal removal has also been extensively studied due to its potential for cost reduction (Li & Tao, 2015). Both Gram-negative and Gram-positive bacteria have shown considerable promise in this application, with effectiveness demonstrated in both viable forms (Rodríguez et al., 2006; Asksonthong et al., 2018; Khashei et al., 2018; Li et al., 2022) and inactive forms (Abd-Alla et al., 2012; Oyetibo et al., 2014; Blanco et al., 2023; Mohapatra et al., 2024).

Naik and Dubey (2013) explained that some indigenous bacteria, when exposed to harsh metal-laden environments, can develop adaptive mechanisms that allow them to tolerate high metal ion concentrations without adversely affecting their growth or metabolic function. In the present study, an indigenous strain of *Serratia marcescens* was isolated from the vicinity of an underground petrol tank and subjected to heavy metal biosorption studies. In bacteria, the cell wall is located externally to the cytoplasmic membrane. It is composed primarily of peptidoglycan, which is a polymer consisting of cross-linked polysaccharide chains and short peptides (Aryal & Liakopoulou-Kyriakides, 2015). In Gram-negative bacteria, the wall is further surrounded by an outer lipid membrane, which contains phospholipids and lipopolysaccharides (Beveridge, 1999). *Serratia marcescens* is a Gram-negative, rod-shaped bacterium belonging to the Enterobacteriaceae family (Cristani et al., 2012). It is facultatively anaerobic and notable for some strains producing a distinctive red pigment called prodigiosin, which carries antifungal, antiprotozoal and antibacterial properties. This bacterium is commonly found in diverse environments, including soil, water, plants and animals, and it can also colonize human respiratory and urinary tracts (Cristani et al., 2012; Lecca-Caballero et al., 2023).

The mechanisms by which bacteria adsorb heavy metals are categorized into two processes. The first, passive biosorption, entails the uptake of metal ions on the cell wall surface. This process is rapid, can be reversible and metabolism-dependent and is also called extracellular binding. The second process is active biosorption, which includes biotransformation and bioaccumulation, which is metabolism-dependent and involves diffusion of the metal ions into the cell membrane. This process is relatively slow and is often referred to as intracellular binding (Veglio & Beolchini, 1997; Li & Tao, 2015). The attachment mechanisms underlying biosorption by bacterial cells may involve physisorption, ion exchange, complexation, cytoplasmic accumulation, and intracellular or extracellular precipitation (Veglio & Beolchini, 1997; Karnwal, 2024). The associated transport mechanism is classified here as cell surface biosorption and diffusion across the cell membrane or intracellular diffusion. Hansda and Kumar (2015) explain that no single

attachment mechanism can fully account for the sorption of heavy metals onto bacteriological cells. Instead, metal binding occurs through one or a combination of physicochemical interactions between the metal ion and the functional groups present on the cell surface. The bacterial cell wall plays a critical role in the passive biosorption of heavy metals. In Gram-negative bacteria, the key biosorption components and some of their functional groups include lipopolysaccharides (LPS) ($–PO_4^{3-}$), outer membrane proteins (–COOH, $–NH_2$), phospholipids ($–PO_4^{3-}$), periplasmic peptidoglycans (–COOH, $–NH_2$) and periplasmic or membrane-associated proteins (–COOH, $–NH_2$). In addition, in biofilm-forming strains, the production of extracellular polymeric substances (EPS) (–OH, –COOH, $–NH_2$, $–PO_4^{3-}$) can enhance metal ion binding (Beveridge, 1999; Hansda & Kumar, 2015; Aryal, 2021).

Serratia marcescens has been previously reported as an efficient biosorbent for heavy metals (Queiroz et al., 2018; Lecca-Caballero et al., 2023). However, many studies have focused on laboratory strains or isolates obtained from relatively low-stress environments, with limited consideration of environmental conditioning or metal tolerance development. In the present study, a strain of *S. marcescens* was isolated from deep subsurface soil collected adjacent to an underground petrol storage facility, an environment characterized by long-term exposure to hydrocarbons and metal stress (Truskewycz et al., 2019). In addition, the isolate was subjected to progressive Cu(II) tolerance induction up to 2.0 mM during the screening, thereby selectively enriching metal-resistant phenotypes. This environmental origin and acclimation strategy distinguish the present isolate from previously reported strains and are reflected in its comparatively higher Cu(II) adsorption capacity (34.4 mg/g). For instance, Díaz et al. (2022) reported on the removal of Cu(II) by *S. marcescens* strain 16, which produced a maximum sorption capacity of 8.6 mg/g with the metal uptake process primarily associated with carbonyl, carboxyl and hydroxyl functional groups as well as amide I and amide II bands. However, the relative contribution of individual uptake mechanisms was not quantitatively resolved. In contrast, the present work aims to integrate kinetic, diffusion, equilibrium and desorption analyses to quantify the contribution of dominant uptake pathways, thereby providing a more comprehensive and mechanistic understanding of metal-biomass interactions.

In this study, *S. marcescens*, isolated from petrol-contaminated soil, was used for the biosorption of Cu(II) and Pb(II) metal ions from synthetic metal-ion solutions. The primary objective was to investigate the underlying transport mechanism using mathematical modelling and elucidate the attachment mechanism through chemical desorption studies. Additionally, biosorption kinetics and equilibrium studies were conducted to inform the optimization of the biosorption process. The findings of this study are intended to evaluate the potential of this metal-resistant *S. marcescens* strain for heavy metal remediation and to provide a foundation for future investigations. For decision-making contexts, strategic environmental assessment is recognized as an enabling instrument for sustainable subsoil use and risk-informed planning, providing a governance frame within which pilot biosorption deployments – for example, at coal-legacy sites – can be scoped and monitored (Karabyn et al., 2022).

2. Materials and Methods

2.1 Determination of metal ion concentration

All the chemicals and reagents used in this study were of analytical grade. Hydrochloric acid, ethylenediaminetetraacetic acid (EDTA) and all other chemical reagents used were

purchased from Merck. Chemical stock solutions of lead (II) nitrate and copper (II) sulphate were prepared using double-distilled water (Corning Mega Pure System of conductivity <5 µS/cm). The concentrations of Cu(II) and Pb(II) ions were determined using an Atomic Absorption Spectrophotometer, Perkin-Elmer AAnalyst 3030B (Perkin-Elmer, Norwalk, CT, USA) equipped with hollow cathode lamps specific to each metal. Throughout the experiments, the solution pH was kept constant using a 0.01M acetate buffer for pH in the range of 5.0-5.75 and measured by a pH meter (Accumet Research-AR10, Fisher Scientific, Pittsburgh, PA, USA). An acetate buffer was used because it provides stable buffering capacity in the mildly acidic range (pH 5.0–5.75) targeted in this study, while minimizing potential interference with Cu(II) and Pb(II) speciation.

2.2 Primary screening and isolation

Bacterial strains were isolated from soil samples collected at a depth of 3.0 m below ground level and 2 m laterally away from an underground petrol storage tank at a fueling station in Arouca, Trinidad. A sample of soil (2.0 g) was added to nutrient broth (DIFCO BACTO), shaken and incubated at 30°C for 24 h. Following the procedure outlined by Philip et al. (1998), a loopful of the culture was transferred to 100 mL of nutrient broth and spiked with 0.25 mM Cu(II) and agitated for 24 h at 30°C. The Cu(II) concentration was progressively increased in 0.25 mM increments, and the process was repeated until a final concentration of 2.0 mM was reached. Serial 10-fold dilutions (10^1-10^6) were prepared, after which aliquots streaked onto nutrient agar plates underwent incubation for 24 h at 35°C. Isolated colonies capable of growing in the presence of Cu(II) were further purified on individual agar slants and screened for Cu(II) biosorption potential. Among the isolates, a strain identified as *S. marcescens* using morphological and biochemical assays exhibited the highest Cu(II) removal efficiency from solution. A biomass sample was subsequently dried at 80°C for 24 h to determine the dry cell weight, yielding an average biomass density of 7.9 g/L. The optical density of *S. marcescens* cells, measured at 580 nm using a spectrophotometer (Milton Roy–Spectronic 601), was empirically calibrated against dry cell weight (Figure 1). Because *S. marcescens* produces the pigmented metabolite prodigiosin, which absorbs near this wavelength, the calibration procedure inherently accounts for pigment contribution, ensuring reliable biomass estimation under the experimental conditions used.

2.3 Batch studies

Bacterial culture was grown in nutrient broth (DIFCO BACTO) for a 24 h period at a temperature of 30°C (Pereira & de Carvalho, 2024), after which the cells were harvested by centrifugation at 6300 rpm for 10 min using a centrifuge (IEC Centra MP4 centrifuge, International Equipment Company, Needham Heights, MA, USA). Biomass collection in sterile test tubes was followed by three washes in 0.9% physiological saline solution. Experiments were carried out in triplicate. All media, glassware, and solutions were sterilized by autoclaving. Solution volumes were accurate to ±0.5 mL. Batch studies were conducted using the parallel method according to EPA OPPTS method 835.1230 (US EPA, 2008). Kinetic studies on metal ion uptake were conducted in a batch reactor with a biosorbent concentration of 1000 mg/L. Each reaction mixture was placed in a 250 mL Erlenmeyer flask and was spiked with a 50 mg/L solution of the target metal ion and agitated for periods up to 90 min. Following biosorption, the biomass was separated by

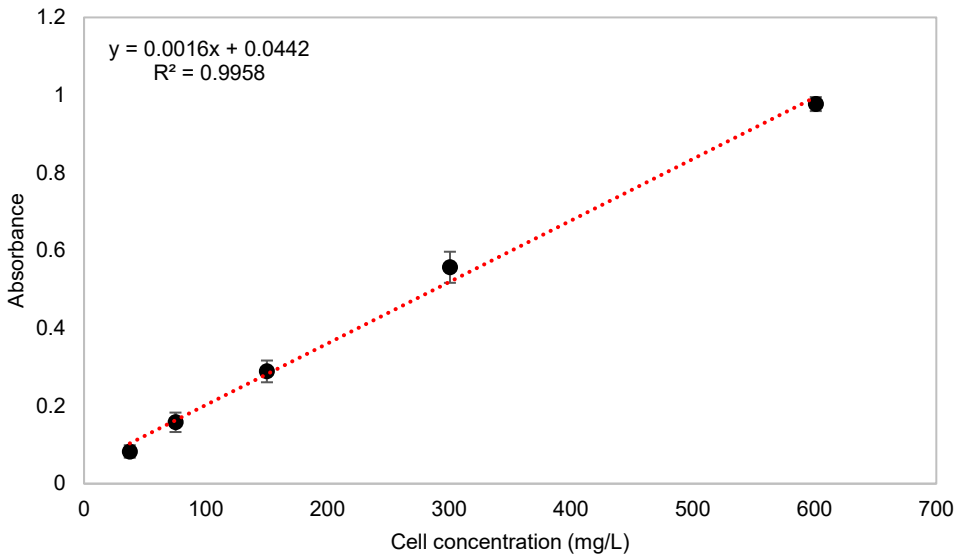


Figure 1. Calibration curve to correlate the optical density of *S. marcescens* cells. Data points represent the mean of triplicate measurements ± standard deviation (SD).

centrifugation at 6300 rpm for 10 min and filtered through a 0.45 µm cellulose nitrate membranes before analysis. The biosorption experiments in this study were restricted to the pH range of 5.0-5.75. This interval was selected to balance biological stability with chemical reliability. At lower pH, the strongly acidic environment can compromise cell viability, while at higher pH (>6.0), Cu(II) and Pb(II) precipitate as hydroxides, making it difficult to distinguish true biosorption from abiotic removal. The maximum uptake of Cu(II) and Pb(II) was observed at pH 5.75 and 5.0, respectively. Equilibrium studies were conducted by varying the initial metal concentration from 10.0 to 80.0 mg/L and at a room temperature of 26±1°C. After 60 min of biosorption, batch desorption studies commenced, with biomass separated and treated with an equivalent volume of desorbing solution (0.1M HCl, 0.1M EDTA, 0.1M $CaCl_2$ or distilled water).

2.4 Controls and quality assurance

Negative controls (metal solutions without biomass) confirmed negligible abiotic loss of Cu(II) and Pb(II). All media and glassware were sterilized prior to use, and sterility was verified by plate incubation of negative controls. Analytical determinations were performed using a Perkin-Elmer AAnalyst 3030B Flame AAS (Perkin-Elmer, Norwalk, CT, USA). Calibration curves were prepared daily with linearity confirmed ($R^2 \geq 0.999$), and mid-range standards were reanalyzed every 10 samples to verify calibration stability. Detection limits, calculated as three times the standard deviation of blank measurements, were 0.02 mg/L for Cu(II) and 0.05 mg/L for Pb(II). Possible interferences from coexisting ions and matrix effects were minimized by maintaining a controlled pH (5.0-5.75) and by verifying recoveries using matrix-matched calibration standards. Standard addition recovery tests confirmed reliability, yielding recoveries between 95% and 103%. All experiments were performed in triplicate.

2.5 Theory

2.5.1 Kinetic and diffusion models

Kinetic analysis was conducted using two kinetic models, namely the pseudo-first-order and pseudo-second-order models, together with two mass-transfer models, the Weber-Morris intraparticle diffusion model and the diffusion-chemisorption (D-C) model. These models were selected because they are widely applied in heavy-metal biosorption studies and, when used in combination, allow discrimination between surface-reaction-controlled sorption and diffusion-controlled transport processes. The pseudo-first-order and pseudo-second-order models describe sorption kinetics governed primarily by surface reactions and chemisorption, whereas the Weber-Morris and D-C models provide mechanistic insight into intraparticle (intracellular) diffusion and the coupled influence of diffusion and chemisorption on the overall sorption rate. All modelling was performed using non-linear regression implemented in CurveExpert© software.

The pseudo-first order model, developed by Lagergren in 1898 (Ho & McKay, 1998a), assumes a first-order rate based on surface reactions and is given as:

$$q_t = q_e(1 - e^{-K_{PFO}t}) \tag{1}$$

Where, q_t (mg/g) is the adsorbate adsorbed per gram of sorbent at any time t; q_e (mg/g) is the solid phase concentration at equilibrium, and K_{PFO} (1/min) is the pseudo-first-order adsorption rate constant.

The pseudo-second order model was developed for the adsorption of divalent metal ions onto peat moss. It assumes the process is chemisorption driven (Ho & McKay, 1998b) and is presented as follows:

$$q_t = \frac{K_{PSO}q_e^2 t}{1 + K_2 q_e t} \tag{2}$$

Where K_{PSO} (g/mg·min) is the pseudo-second-order rate constant.

The Weber and Morris (1963) intraparticle diffusion model is given as:

$$q_t = K_{id}\left(t^{\frac{1}{2}}\right) + c \tag{3}$$

Where K_{id} (mg/g·$t^{1/2}$) is the rate constant of intraparticle transport.

The diffusion-chemisorption model, developed by Sutherland (2004), simulates the sorption of heavy metals onto heterogeneous media and assumes that both diffusion and chemisorption govern the adsorption process (Sutherland & Venkobachar, 2010). A key assumption in the model is the exponent value of n = 0.5, which signifies a parabolic time dependence and is characteristic of systems where intraparticle diffusion governs the rate-limiting step (Sutherland, 2025). The model is presented as follows:

$$q_t = \frac{q_e K_{DC} t^{0.5}}{q_e + K_{DC} t^{0.5}} \tag{4}$$

The initial sorption rate is given as:

$$k_i = \frac{{K_{DC}}^2}{q_e} \tag{5}$$

The reaction time to achieve any specified level of sorbent saturation is represented as:

$$t_x = [W - 1]^2 \left[\frac{q_e}{K_{DC}}\right]^2 \tag{6}$$

and

$$W = \frac{q_e}{q_e - q_t} \tag{7}$$

To determine the half-time of the reaction, i.e. when $q_t = 0.5q_e$, Equation 6 becomes:

$$t_{1/2} = \left[\frac{q_e}{K_{DC}}\right]^2 \tag{8}$$

The intraparticle diffusion influencing factor is given as:

$$R_{DC} = \frac{q_e}{K_{DC} t_{ref}^{0.5}} \tag{9}$$

Where K_{DC} (mg/g·$t^{0.5}$) is the diffusion-chemisorption overall rate constant, k_i (mg/g·t) is the initial reaction rate; $t_{1/2}$ is the reaction half-time, t_x is the time required to achieve any specific level of adsorbent saturation; R_{DC} is the solid-phase mass transfer index (Table 1) and t_{ref} is the longest experimental time in an adsorption system.

The characteristic curve can be generated by a plot of T vs. Q_t using the following equation:

$$Q_t = \frac{T\,[1+R_{DC}]}{T+R_{DC}} \tag{10}$$

Where T represents the elapsed time in the adsorption process, and Q_t represents the fractional progress toward equilibrium.

$$Q_t = \frac{q_t}{q_{ref}} \tag{11}$$

$$T = \frac{t^{0.5}}{t_{ref}^{0.5}} \tag{12}$$

Figure 4 illustrates the characteristic curve, which was plotted using equation (10). By applying fixed R_{DC} values (< 0.01, 0.1, 1, and >1), the corresponding Q_t values can be determined for any T-value within the range 0 to 1. Table 1 summarizes the classification of mechanistic behavior based on the D-C model using the solid-phase mass-transfer index (R_{DC}).

Table 1. Mechanistic behavior based on the diffusion-chemisorption kinetic model and the limits of the solid-phase mass transfer index (R_{DC})

R_{DC} Value	Shape of Kinetic Curve	Influence of Intraparticle Diffusion and Chemisorption	Type
$R_{DC} \geq 1$	Slightly Curve	Significant Influence of Intraparticle Diffusion	I
$0.1 \leq R_{DC} < 1$	Moderately Curved	Moderate Influence of Intraparticle Diffusion	II
$0.01 \leq R_{DC} < 0.1$	Largely Curved	Low Influence of Intraparticle Diffusion	III
$R_{DC} < 0.01$	Pseudo-Rectangular	Insignificant Influence of Intraparticle Diffusion	IV

Note. R_{DC} = solid-phase mass transfer index

2.5.2 Equilibrium models

Equilibrium modelling was carried out using the Langmuir and the Freundlich isotherms. The Langmuir isotherm model is based on the assumption that all adsorption sites are energetically identical and can accommodate only one adsorbate molecule each (Langmuir, 1918). Thus, the process results in the formation of monolayer coverage and is associated with a chemisorption-driven process. The Freundlich isotherm, introduced in 1906, describes reversible and non-ideal adsorption behavior (Freundlich, 1907). It accounts for surface heterogeneity and reflects the variation in adsorption site energies and their distribution (Ayawei et al., 2017). The non-linear forms of the model are presented in equations 13 and 14.

$$q_e = \frac{q_m K_L C_e}{1 + K_L C_e} \tag{13}$$

$$q_e = K_F C_e^{1/n} \tag{14}$$

Where q_m (mg/g) is the monolayer adsorption capacity; C_e (mg/L) is the final concentration of ions in solution; K_L (L/mg) is the Langmuir's constant related to apparent heat change; and K_F (L/mg) is the Freundlich constant related to adsorption affinity.

3. Results and Discussion

3.1 Kinetic characteristics of Cu(II) and Pb(II) biosorption

The fitting parameters for the pseudo-first-order, the pseudo-second-order, the diffusion-chemisorption and the intraparticle diffusion models are presented in Table 2. The data were well represented for both the biosorption of Cu(II) and Pb(II) by the pseudo-first-order model, yielding coefficients of determination (R^2) of 0.9966 and 0.9975, respectively. This assessment is also supported by the close agreement between experimental and calculated q_e values. The model is based on the assumption that the reaction follows a

first-order rate and is influenced by surface reaction. Comparable findings were reported by Masoumi et al. (2016), who observed similar kinetic behavior for the biosorption of Pb(II) by *Curtobacterium* sp. Analysis of the primary kinetic curves as a function of time revealed a biphasic sorption pattern (Figure 2), exhibiting a rapid initial uptake followed by a gradual approach to equilibrium. The time to reach equilibrium for both Cu(II) and Pb(II) was within 60 min, as successive time points showed no substantial variation in the amount adsorbed. The attainment of equilibrium at this time was further supported by kinetic model fitting, which indicated that equilibrium was achieved in around 60 min. Accordingly, all subsequent equilibrium experiments were conducted using a 60-minute contact time. The rate constants derived from the pseudo-first-order model (K_{PFO}) indicated that Pb(II) had a slower kinetic response, with an overall rate approximately 40% lower than that of Cu(II). Further insights were obtained from the initial rate (k_i) estimated by the diffusion-chemisorption model. It was noted that the initial rate for Cu(II) uptake was seven times higher than that of Pb(II). This faster initial interaction may have been the result of higher surface affinity for Cu(II) ions or transport limitations in the case of Pb(II) ions. Another useful kinetic descriptor was the time required to achieve a particular level of biosorbent saturation. For instance, the reaction half-time ($t_{1/2}$), calculated using Eqs. 6-8, showed that Cu(II) uptake by *S. marcescens* reached 50% of its capacity in just 2.2 min, whereas Pb(II) required 13.9 min to reach the same saturation level (Table 3). This metric provided a practical basis for comparing system responsiveness under varying treatment conditions. From an operational perspective, the analysis presented in Table 3 enables a trade-off assessment between treatment efficiency and processing time. For example, achieving 90% saturation in the biosorption of Pb(II) requires approximately five times the duration needed to attain 80% saturation. These comparisons demonstrate how kinetic descriptors, such as half-time and fractional uptake, can guide process optimization by balancing sorbent utilization and contact time.

Table 2. Comparison of kinetic models using non-linear regression to simulate Cu(II) and Pb(II) uptake by *S. marcescens*

Model	Parameters	Cu(II)	Pb(II)
Lagergren pseudo-first-order	q_e	24.651	16.538
	K_{PFO}	0.216	0.133
	R^2	0.9966	0.9975
Pseudo-second-order	q_e	26.314	18.446
	K_{PSO}	0.0143	0.01
	R^2	0.9912	0.9960
Diffusion-chemisorption	q_e	30.147	25.175
	K_{DC}	20.136	6.763
	R^2	0.9805	0.9683
	k_i	13.449	1.817
	R_{DC}	0.156	0.392
Intraparticle diffusion	K_{ID}	2.264	1.7552
	c	9.003	3.878
	R^2	0.6542	0.7980

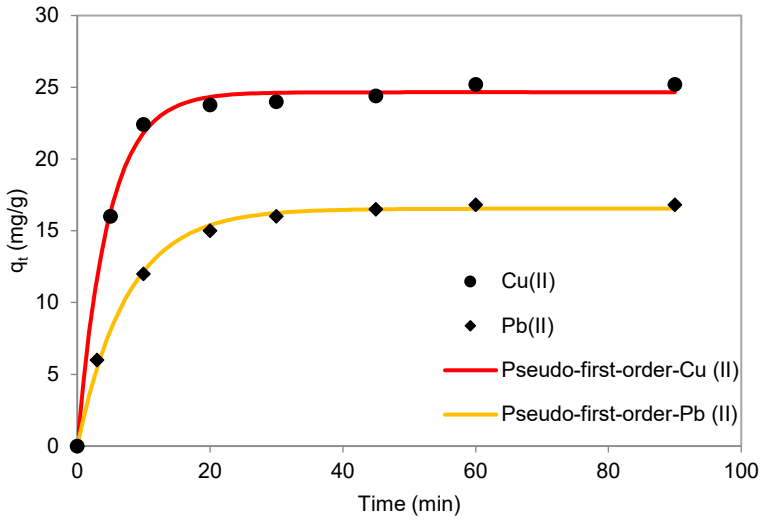


Figure 2. Pseudo-first-order kinetic model simulation of Cu(II) and Pb(II) uptake by *S. marcescens*. Data points represent mean values from triplicate runs±standard deviation (SD).

Table 3. Relationship between *S. marcescens* coverage and operating time for Cu(II) and Pb (II) uptake

Fractional biosorption, X	q_t/q_e=0.5	q_t/q_e=0.6	q_t/q_e=0.8	q_t/q_e=0.9	q_t/q_e=0.95	q_t/q_e=0.97
Contaminant	$t_{0.5}$ (min)	$t_{0.6}$ (min)	$t_{0.8}$ (min)	$t_{0.9}$ (min)	$t_{0.95}$ (min)	$t_{0.97}$ (min)
Cu(II)	2.20	4.95	35.23	178.35	794.87	2301.93
Pb(II)	13.86	31.18	221.73	1122.49	5002.71	14487.68

3.2 Elucidation of transport mechanisms

To elucidate the underlying transport mechanisms governing the biosorption process, both the Weber and Morris intraparticle diffusion model and the diffusion-chemisorption (D-C) model were applied to the kinetic data for Cu(II) and Pb(II) biosorption. Using the Weber and Morris model, plots of q_t vs. $t^{0.5}$ for Cu(II) and Pb(II) reveal multilinear trends (Figure 3), indicative of the presence of more than one rate-limiting step. According to Wu et al. (2009), the Weber and Morris model characterizes sorption as a sequence of distinct phases: (i) an initial external surface biosorption, (ii) a gradual intraparticle diffusion phase, and (iii) a final equilibrium stage, where the diffusion of sorbate molecules transitions from macropores to micropores at a slower rate. In the present study, the plots for both Cu(II) and Pb(II) clearly exhibited three distinct linear regions corresponding to rapid external surface biosorption followed by a gradual sorption step that likely reflected the slower diffusion through the cell membrane. In both instances, the reactions achieved equilibrium during the second stage. This was reflected by the observed plateauing in the third segment (Figure 3). Additionally, the near-intersection of both curves with the origin indicated that the influence of film diffusion was negligible (Sutherland, 2025). It is

noteworthy that although the Weber-Morris intraparticle diffusion model theoretically distinguishes three sequential stages, the transitions between these phases are often gradual rather than sharply delineated. In the present study (Figure 3), the uptake profile shows a rapid initial stage followed by a slower diffusion-controlled region before levelling off toward equilibrium. These boundaries are approximate and should be interpreted cautiously, as overlapping processes may operate simultaneously. Consistent with literature reports, the Weber-Morris model here is best regarded as providing indicative evidence of diffusion contributions rather than a precise partitioning of kinetic phases.

It is important to recognize that in practical systems, transport mechanisms may not occur in discrete, isolated stages, but can overlap and act concurrently. To further evaluate the role of intraparticle diffusion, which is interpreted here as intracellular or membrane-associated transport, the D-C model was applied. This model offers quantitative insight into the extent to which diffusion influences overall sorption kinetics. The D-C model provided a good fit to the kinetic data, with coefficients of determination R^2 of 0.9800 for Cu(II) and 0.9683 for Pb(II), respectively. The corresponding values of the intraparticle diffusion influencing factor, represented by the solid-phase mass transfer index (R_{DC}), were calculated using equation 9 and presented in Table 2. R_{DC} is an indicative parameter used to reflect the relative contribution of diffusion resistance. The values of R_{DC} were determined to be 0.156 for Cu(II) and 0.392 for Pb(II). Both values fall within the range $0.1 \leq R_{DC} < 1$, which denotes moderate control by intraparticle diffusion (Table 1). The higher R_{DC} value for Pb(II) suggests a more pronounced influence of intracellular diffusion over the entire biosorption process compared to Cu(II). The characteristic D-C curves shown in Figure 4, which were developed using equations 10-12 further support this inference. Visually, the Pb(II) curve (represented by a yellow continuous line) reflects a stronger diffusion contribution throughout the biosorption duration. Additionally, the slopes of the second linear segments (curves 1b and 2b) from the Weber and Morris plots, which correspond to the intraparticle diffusion phase, were calculated as 0.5504 for Cu(II) and 0.5311 for Pb(II). The slope values are comparable, and therefore, the longer time interval over which intracellular diffusion was the dominant rate-limiting step in Cu(II) uptake may not have been due to its strong influence, but due to the insignificant influence of surface biosorption over this period. Consequently, it can be inferred that while intracellular diffusion dominated the reaction longer for Cu(II), its relative contribution to the overall biosorption process was greater for Pb(II), as evidenced by the higher R_{DC} value. As such, the Weber and Morris curve does not depict when intraparticle diffusion begins and ends, but the period over which it dominates in the reaction. Further, it does not quantify its influence on the overall biosorption process. In contrast, the D-C model provided a more integrated perspective, indicating that for Pb(II), intracellular diffusion exerted a greater influence throughout the biosorption process.

3.3 Equilibrium sorption characteristics of Cu(II) and Pb(II)

Table 4 presents the goodness of fit for each model and the corresponding parameters obtained through non-linear regression for the biosorption of Cu(II) and Pb(II) by *S. marcescens*. The equilibrium data were well represented by both the Langmuir and the Freundlich models (Figure 5). However, in both instances, the Freundlich model produced a slightly higher R^2 value. Quiton et al. (2018) explained that in such situations, the active sites present the characteristics of both heterogeneous energetic distribution and monolayer formation. Similarly, Zakeri et al. (2010) reported that the biosorption of radium

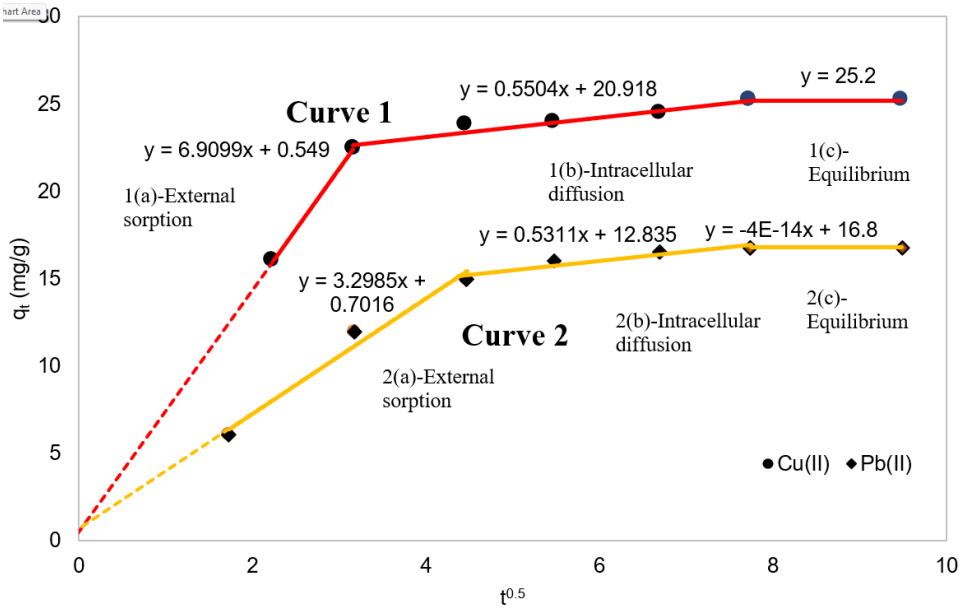


Figure 3. Plot of the Weber and Morris intraparticle diffusion model for Cu(II) and Pb(II) uptake by *S. marcescens*

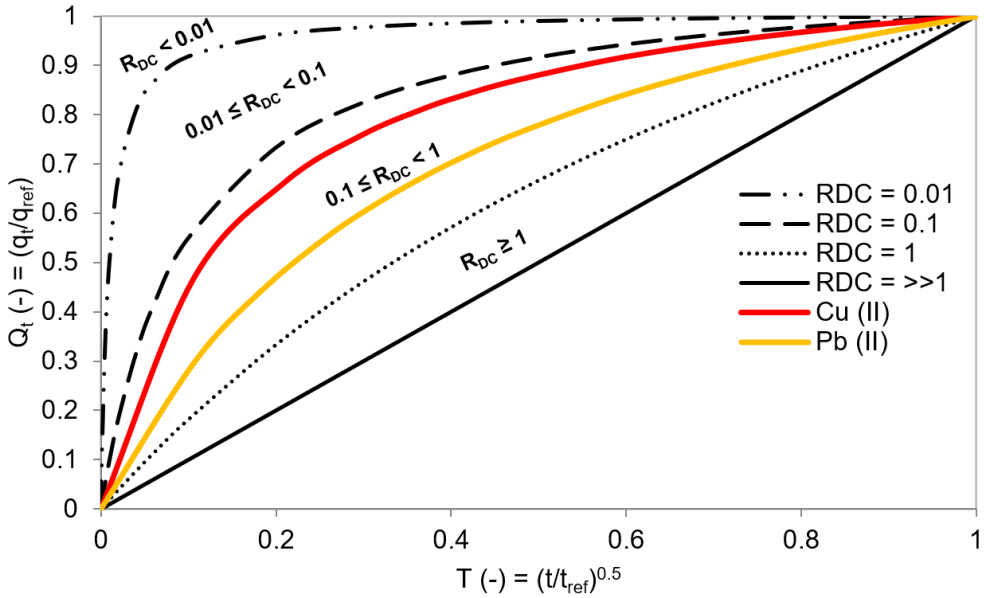


Figure 4. Typical characteristic curves of the diffusion-chemisorption model with curves of Cu(II) and Pb(II) uptake by *S. marcescens* overlayed

Table 4. Comparison of isotherm models using non-linear regression to simulate Cu(II) and Pb(II) uptake by *S. marcescens*

Model	Parameters	Cu(II)	Pb(II)
Freundlich isotherm	K_F	4.554	3.960
	n	2.325	2.600
	R^2	0.9983	0.9953
Langmuir isotherm	q_m	34.354	22.186
	K_L	0.0507	0.076
	R^2	0.9920	0.9925

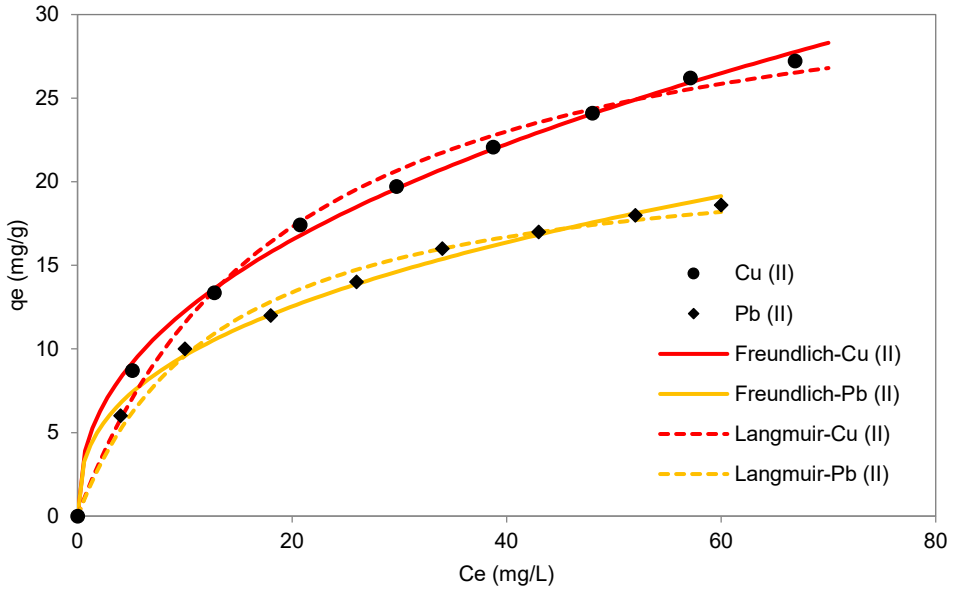


Figure 5. Equilibrium isotherm model simulations against experimental biosorption data for Cu(II) and Pb(II)

by a *Serratia sp.* was also best represented by both isotherms, with the Freundlich producing a higher R^2 value. Chou et al. (2010) explained that the Freundlich constant (n) equals unity when the adsorbent sites have equal affinity. For values of $n < 1$, the process is physical in nature, while $n > 1$ implies a chemisorption-dominant process. In the modelling of Cu(II) and Pb(II), the value of n was > 1, implying a dominance of chemically mediated processes. According to the Langmuir model, a monolayer sorption capacity of 34.4 and 22.2 mg/g was observed at a temperature of 26°C and a reaction time of 60 min. The higher Cu(II) adsorption capacity may be partly attributed to the Cu(II) tolerance-induction protocol used during strain isolation, which likely promoted adaptive responses and enhanced affinity toward Cu(II), whereas Pb(II) was not involved in the selective acclimation process. In addition, the smaller hydrated radius of Cu(II) may have further enhanced diffusion and binding site accessibility, whereas the higher atomic mass of Pb(II)

could have reduced ion mobility. Similar observations were reported by Cheng et al. (2012) for magnetotactic bacteria's adsorption of heavy metals. Table 5 compares the performance of *S. marcescens* with that of other bacterial biosorbents reported in the literature for the removal of Cu(II) and Pb(II). In both cases, *S. marcescens* exhibited biosorption efficiency comparable to that of other bacterial biomass. It should also be noted that reported biosorption capacities vary with experimental conditions such as pH, temperature, initial concentration and biomass pretreatment; therefore, the values in Table 5 are presented as general indicators rather than standardized benchmarks.

Table 5. Comparison of Cu(II) and Pb(II) monolayer biosorption capacity based on Langmuir's isotherm with various bacterial biomass reported in the literature

Biosorbent	Contaminant	Initial Concentration Range (mg/L)	Adsorption Capacity (mg/g)	Reference
Shewanella putrefaciens	Cu(II)	10-500	45.0	(Chubar et al., 2008)
Bacillus stercoris	Cu(II)	50-500	35.1	(Majhi et al., 2023)
Pseudomonas alcaliphila	Cu(II)	50-500	31.1	(Majhi et al., 2023)
Bacillus pumilus	Cu(II)	0-100	11.9	(Danial & Dardir, 2023)
Bacillus subtilis	Cu(II)	0-100	19.9	(Danial & Dardir, 2023)
Lactobacillus casei	Cu(II)	-	23.2	(Endo & Aoyagi, 2018)
Serratia marcescens	Cu(II)	10-80	34.4	*This study*
Pseudomonas sp. LKS06	Pb(II)	10-300	77.8	(Huang & Liu,2013)
Pontederia rotundifolia	Pb(II)	5-50	7.1	(de Freitas et al., 2018)
Salvinia biloba	Pb(II)	5-50	23.2	(de Freitas et al., 2018)
Lactobacillus brevis	Pb(II)	10-200	53.6	(Dai et al., 2019)
Bacillus sp. PZ-1	Pb(II)	50-500	9.3	(Ren et al., 2015)
Serratia marcescens	Pb(II)	10-80	22.2	*This study*

3.4 Desorption studies

To elucidate the attachment mechanisms governing Cu(II) biosorption by *S. marcescens*, desorption studies were conducted using four eluents, viz., distilled water, calcium chloride ($CaCl_2$), ethylenediaminetetraacetic acid (EDTA) and hydrochloric acid (HCl). These eluent washes were administered individually and sequentially. Each eluent was selected to target particular binding interactions between Cu(II) ions and the *Serratia sp.* Ions released as a result of distilled water wash are usually associated with physical adsorption, where the ions are held due to low-energy weak surface interactions (Ahammad et al., 2021). The $CaCl_2$ wash introduces competing ions of the same valency as Cu(II) but with an increased

concentration, forcing the exchange of ions from sites involved in electrostatic binding (Wolf et al. 1977). EDTA, a chelating agent known to form complexes with metal ions, was employed to disrupt stronger chemical interactions, particularly covalent and coordination bonds (Sutherland & Venkobachar, 2020). The harsh HCl wash was applied as a strong acid capable of lysing bacterial cells. Through compromise of the structural integrity of the microbial cells, Cu(II) ions held through bioaccumulation can be released into solution (Sutherland et al., 2023).

To perform individual desorption, four bacteriological samples were first subjected to biosorption of Cu(II) ions. Each sample was then treated with different eluents to determine the maximum amount of Cu(II) ions desorbed by each agent. The sequential desorption test was performed by exposing the same *S. marcescens* sample to each of the four eluents to assess the contribution of each binding mechanism. Following the biosorption of Cu(II) ions (initial concentration of 75 mg/L), the cells were subjected to a distilled water wash under agitation for 60 min. The sample was then separated by centrifugation at 6300 rpm for 10 min. The bacteriological cells were recovered, and the process was repeated using a 0.1 M $CaCl_2$ solution, followed by 0.1 M EDTA and finally 0.1 M HCl. Mass balance calculations confirmed that 100% of the adsorbed Cu(II) was recovered, demonstrating excellent agreement between adsorption and desorption data and confirming the reliability of the results. The results of the sequential desorption are presented in Figure 6. The distilled water wash released 0.9 % of the sorbed Cu(II) ions, which suggested that this fraction may have been held via weak physical interactions. The subsequent $CaCl_2$ wash released 47.3 % of the sorbed ions, which may indicate an ion exchange mechanism. The EDTA elution resulted in the release of a further 47.3 % of the sorbed Cu(II) ions. This percentage of the uptake was consistent with chemical bonding. Finally, the HCl wash released the remaining 4.5% of the bound Cu(II) ions, which may indicate bioaccumulated ions, as the HCl wash is known to disrupt bacterial cell membranes and internal structures. The cumulative percentages of Cu(II) released by distilled water, $CaCl_2$, EDTA and finally HCl added to the total amount initially adsorbed, within the ±2% experimental uncertainty of the atomic absorption measurements. The individual desorption test confirmed that distilled water, $CaCl_2$, EDTA and HCl released 0.9%, 48.5%, 95.5% and 100%, respectively. These findings indicate that the $CaCl_2$ wash could release ions held by both physisorption and ion exchange. Further, the EDTA wash released 95.5 %, which accounted for Cu(II) ions held by physisorption, ion exchange and complexation. The complete desorption observed with HCl suggests that this wash could release all bound Cu(II) ions, including those held via bioaccumulation within the cell matrix. Figure 7 presents the desorption kinetics data. Due to a rapid release of metal ions, within the first 2 min of the desorption, equilibrium was achieved by distilled water, $CaCl_2$ and HCl. However, elution by EDTA required approximately 20 min to achieve desorption equilibrium. The distilled water, $CaCl_2$ and HCl rapid release of metal ions further suggested that the associated binding of Cu(II) may have been through a combination of weak and easily reversible bonding, such as physisorption and ion-exchange. Further, acid-induced cell lysis by HCl would break physical and chemical bonds and release bioaccumulated ions. EDTA required 20 min to reach desorption equilibrium, indicating a slower desorption process. This delayed process may have been due to the complexity of disrupting coordination and covalent bonds, as well as the formation of metal-ligand complexes by the chelating agent, which may have occurred more slowly than through simple ion displacement or physical release mechanisms. In a large proportion of biosorption studies, binding mechanisms are commonly inferred from single-step desorption using a single eluent, such as EDTA to indicate complexation or mineral acids to suggest intracellular retention, or from qualitative shifts in FTIR spectra. While such

approaches can indicate which interactions may be involved, they generally do not allow the relative contributions of different mechanisms to be quantified. It is emphasized that while the differential desorption responses provide useful indications of possible binding mechanisms, such results are indirect and should be viewed as supportive evidence rather than conclusive proof; definitive confirmation would require complementary spectroscopic or microscopic analyses.

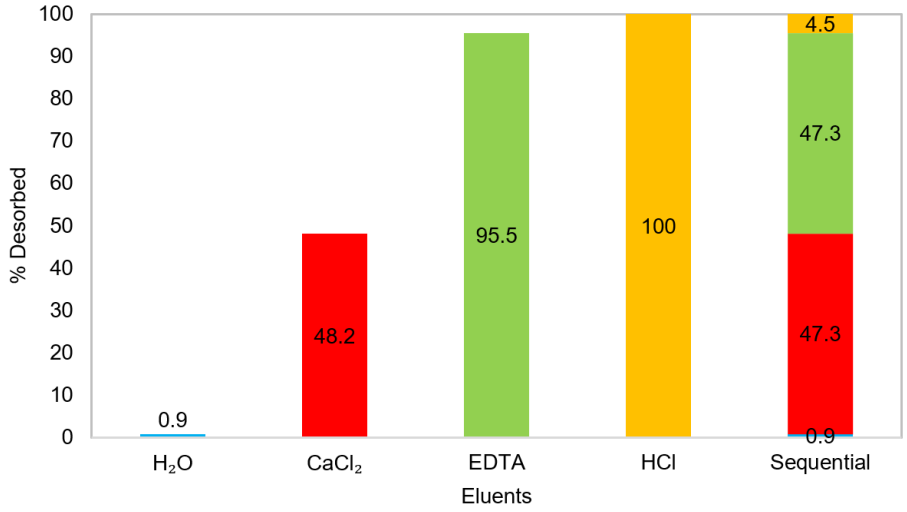


Figure 6. Cu(II) sequential and individual desorption from *S. marcescens* using various eluents. Bar colors correspond to the eluents tested: distilled water, $CaCl_2$, EDTA and HCl.

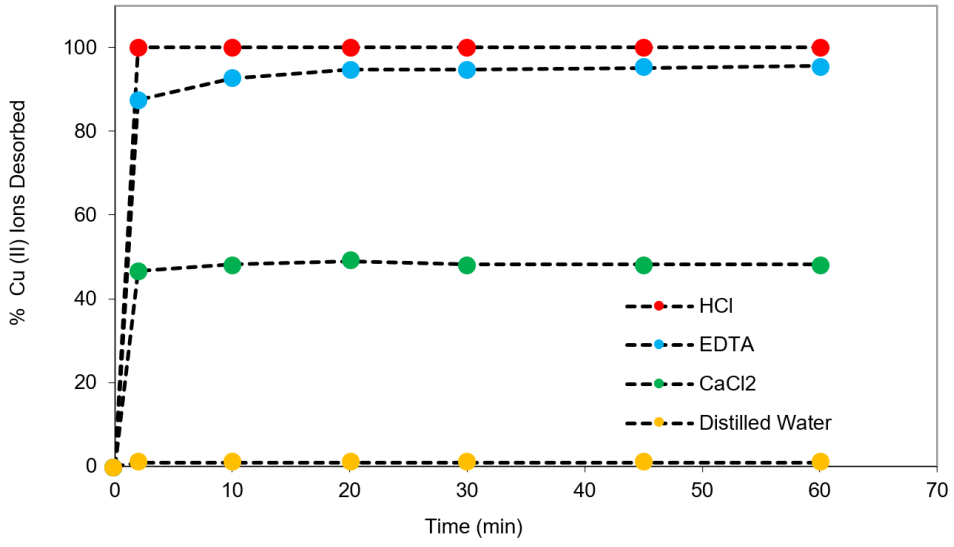


Figure 7. Desorption kinetics of Cu(II) release from *S. marcescens* using various eluents

3.5 Limitations and future work

This study provides important insights into the biosorption of Cu(II) and Pb(II) by *S. marcescens*. Experimental conditions were restricted to room temperature (26±1°C) and a narrow pH range (5.0-5.75) to maintain microbial viability and minimize precipitation. Broader investigations across environmental conditions, including thermodynamic analyses (ΔG°, ΔH°, ΔS°) and assessments of the effects of competing ions and organic matter, will further aid in process optimization. While desorption experiments offered valuable indications of the dominant binding mechanisms, further confirmation through direct spectroscopic and microscopic techniques is warranted. Methods such as FTIR, XPS, TEM, and SEM-EDX could enable identification of functional groups and metal-binding sites, strengthening the linkage between observed desorption trends and underlying molecular interactions. The concentration range tested (10-80 mg/L) was suitable for contaminated effluents; however, future work should be extended to include both trace levels and higher levels to broaden applicability. Finally, this study was confined to controlled laboratory conditions; validation under real wastewater matrices, as well as scale-up and cost-benefit assessments, will be essential for practical implementation.

4. Conclusions

In this study, a metal-tolerant strain of *S. marcescens* was isolated from soil near a fuel storage tank and employed for the biosorption of Cu(II) and Pb(II) from aqueous solution. Kinetic analysis revealed that the pseudo-first-order model provided the best fit for simulating the biosorption of both metal ions. The model suggested surface sorption as an influencing mechanism. To further elucidate the underlying transport mechanisms, the Weber and Morris intraparticle diffusion model and the diffusion-chemisorption (D-C) model were applied. The models provided complementary insight into the transport mechanisms and revealed that surface biosorption and intracellular diffusion were key mechanisms involved in the process. The Weber and Morris plots revealed the existence of multiple sorption phases, with distinct diffusion-dominated regions. The D-C model's solid-phase mass transfer index (R_{DC}) indicated that the biosorption of both metals fell within the range associated with moderate intraparticle diffusion control, with a greater influence of intracellular diffusion in the biosorption of Pb(II) (R_{DC} = 0.392) compared to Cu(II) (R_{DC} = 0.156). Equilibrium modelling of Cu(II) and Pb(II) biosorption demonstrated that both the Langmuir and the Freundlich isotherms provided a good fit to the experimental data, with the Freundlich model yielding slightly higher coefficients of determination. This suggests that the biosorption process involves a combination of monolayer coverage and heterogeneous surface interactions. The Freundlich constant of n>1 for both metals further supports the predominance of chemisorption mechanisms. Monolayer sorption capacities estimated from the Langmuir model were 34.4 mg/g for Cu(II) and 22.2 mg/g for Pb(II) within 60 min and at a temperature of 26°C. Desorption studies using distilled water, $CaCl_2$, EDTA, and HCl provided valuable insights into the mechanisms governing Cu(II) attachment to *S. marcescens*. The negligible desorption observed with distilled water (0.9%) suggested minimal contribution from weak physical interactions. $CaCl_2$ and EDTA each released 47.3% of the sorbed Cu(II), suggesting a marked involvement of ion-exchange and chemisorption mechanisms, respectively. The final 4.5% recovered using HCl was consistent with bioaccumulated Cu(II) ions within the cell matrix. The desorption studies demonstrated that Cu(II) ions involved multiple mechanisms, including physisorption, ion exchange, chemisorption and intracellular binding. Kinetic desorption

profiles further demonstrated a rapid equilibrium for water, $CaCl_2$, and HCl (≤2 min) but slower release for EDTA (~20 min), which may have been due to the slow process of disrupting complex bonds. The integration of kinetic, equilibrium, and desorption studies not only provided a comprehensive understanding of transport and attachment mechanisms but also linked measurable operating times with recoverable capacities and regeneration routes. Most notably, by attributing specific desorbing agents to distinct binding interactions, the approach provides mechanistic clarity and functions as an independent validation of standard mechanistic analyses, while simultaneously identifying and ranking the relative importance of active mechanisms. This validated understanding enables more confident scale-up of biosorption systems and can guide the development of effective regeneration strategies. Ultimately, it strengthens the reliability of biosorption as a cost-effective and sustainable technology for heavy-metal remediation.

5. Authors' Contributions

Clint Sutherland: study conception and design, investigation, analysis and interpretation of results and manuscript preparation. Vasyl Karabyn: analyzed data; supplemented and edited the paper.

ORCID

Clint Sutherland https://orcid.org/0000-0002-5569-325X

Vasyl Karabyn https://orcid.org/0000-0002-8337-5355

6. Conflicts of Interest

The authors declare that there is no conflict of interest in this study.

References

Abd-Alla, M. H., Morsy, F. M., El-Enany, A.-W. E., & Ohyama, T. (2012). Isolation and characterization of a heavy-metal-resistant isolate of *Rhizobium leguminosarum* bv. viciae potentially applicable for biosorption of Cd^{2+} and Co^{2+}. *Journal of International Biodeterioration and Biodegradation*, *67*, 48-55. https://doi.org/10.1016/j.ibiod.2011.10.008

Ahammad, N. A., Zulkifli, M. A., Ahmad, M. A., Hameed, B. H., & Din, A. M. (2021). Desorption of chloramphenicol from ordered mesoporous carbon–alginate beads: Effects of operating parameters, and isotherm, kinetics, and regeneration studies. *Journal of Environmental Chemical Engineering*, *9*(1), Article 105015. https://doi.org/10.1016/j.jece.2020.105015

Al-Bahathy, I. A. A., Al-Janabi, Z. Z., Al-Hassany, J. S., Majeed, O. S., & Naje, A. S. (2024). Environmental assessment of sediment quality for the Main Outfall Drain and Al-Sanaf Marsh. *Ecological Engineering and Environmental Technology*, *25*(4), 188-196. https://doi.org/10.12912/27197050/183645

Aryal, M. (2021). A comprehensive study on the bacterial biosorption of heavy metals: Materials, performances, mechanisms, and mathematical modellings. *Reviews in Chemical Engineering*, *37*(6), 715-754. https://doi.org/10.1515/revce-2019-0016

Aryal, M., & Liakopoulou-Kyriakides, M. (2015). Bioremoval of heavy metals by bacterial biomass. *Environmental Monitoring and Assessment*, *187*(1), Article 4173. https://doi.org/10.1007/s10661-014-4173-z

Ashraf, A., Dutta, J., Farooq, A., Rafatullah, M., Pal, K., & Kyzas, G. Z. (2024). Chitosan-based materials for heavy metal adsorption: Recent advancements, challenges and limitations. *Journal of Molecular Structure*, *1309*, Article 138225. https://doi.org/10.1016/j.molstruc.2024.138225

Asksonthong, R., Siripongvutikorn, S., & Usawakesmanee, W. (2018). Heavy metal removal ability of *Halomonas elongata* and *Tetragenococcus halophilus* in a media model system as affected by pH and incubation time. *International Food Research Journal*, *25*(1), 234-240.

Ayawei, N., Ebelegi, A. N., & Wankasi, D. (2017). Modelling and interpretation of adsorption isotherms. *Journal of Chemistry*, *2017*, Article 3039817. https://doi.org/10.1155/2017/3039817

Beveridge, T. J. (1999). Structures of Gram-negative cell walls and their derived membrane vesicles. *Journal of Bacteriology*, *181*(16), 4725-4733. https://doi.org/10.1128/JB.181.16.4725-4733.1999

Bharti, R., & Sharma, R. (2022). Effect of heavy metals: An overview. *Materials Today: Proceedings*, *51*, 880-885. https://doi.org/10.1016/j.matpr.2021.06.278

Blanco, A., Sampedro, M. A., Sanz, B., Llama, M. J., & Serra, J. L. (2023). Immobilization of non-viable cyanobacteria and their use for heavy metal adsorption from water. In G. Sánchez & E. Hernández (Eds.), *Environmental biotechnology and cleaner bioprocesses* (pp. 135-153). CRC Press. https://doi.org/10.1201/9780429327761-9

Chakraborty, R., Asthana, A., Singh, A. K., Jain, B., & Susan, A. B. H. (2022). Adsorption of heavy metal ions by various low-cost adsorbents: A review. *International Journal of Environmental Analytical Chemistry*, *102*(2), 342-379. https://doi.org/10.1080/03067319.2020.1722811

Cheng, H., Song, H., & Cheng, F. (2012). The effect of ion charge-mass ratio on adsorption of heavy metals on magnetotactic bacteria. *African Journal of Microbiology Research*, *6*(50), 7564-7571.

Chou, W.-L., Wang, C.-T., Chang, W.-C., & Chang, S. Y. (2010). Adsorption treatment of oxide chemical mechanical polishing wastewater from a semiconductor manufacturing plant by electrocoagulation. *Journal of Hazardous Materials*, *18*0(1-3), 217-224. https://doi.org/10.1016/j.jhazmat.2010.04.017

Chubar, N., Behrends, T., & Van Cappellen, P. (2008). Biosorption of metals (Cu^{2+}, Zn^{2+}) and anions (F^{-}, $H_2PO_4^{-}$) by viable and autoclaved cells of the Gram-negative bacterium *Shewanella putrefaciens*. *Colloids and Surfaces B: Biointerfaces*, *65*(1), 126-133. https://doi.org/10.1016/j.colsurfb.2008.03.006

Cristani, M., Naccari, C., Nostro, A., Pizzimenti, A., Trombetta, D., & Pizzimenti, F. (2012). Possible use of *Serratia marcescens* in toxic metal biosorption (removal). *Environmental Science and Pollution Research*, *19*(1), 161-168. https://doi.org/10.1007/s11356-011-0539-8

Cunningham, S. A. (2005). Incident, accident, catastrophe: Cyanide on the Danube. *Disasters*, *29*(2), 99-128. https://doi.org/10.1111/j.0361-3666.2005.00276.x

Dai, Q. H., Bian, X. Y., Li, R., Jiang, C. B., Ge, J. M., Li, B. L., & Ou, J. (2019). Biosorption of lead (II) from aqueous solution by lactic acid bacteria. *Water Science and Technology*, *79*(4), 627-634.

Danial, A. W., & Dardir, F. M. (2023). Copper biosorption by *Bacillus pumilus* OQ931870 and *Bacillus subtilis* OQ931871 isolated from Wadi Nakheil, Red Sea, Egypt. *Microbial Cell Factories*, *22*(1), Article 152. https://doi.org/10.1186/s12934-023-02166-3

de Freitas, F., Battirola, L. D., & de Andrade, R. L. T. (2018). Adsorption of Cu2+ and Pb2+ ions by *Pontederia rotundifolia* (L. f.) (Pontederiaceae) and *Salvinia biloba* Raddi (Salviniaceae) biomass. *Water, Air, and Soil Pollution*, *229*, Article 349. https://doi.org/10.1007/s11270-018-4005-9

Díaz, A., Marrero, J., Cabrera, G., Coto, O., & Gómez, J. M. (2022). Biosorption of nickel, cobalt, zinc and copper ions by *Serratia marcescens* strain 16 in mono and multimetallic systems. *Biodegradation*, *33*(1), 33-43.

Endo, R., & Aoyagi, H. (2018). Adsorption preference for divalent metal ions by *Lactobacillus casei* JCM1134. *Applied Microbiology and Biotechnology*, *102*(14), 6155-6162. https://doi.org/10.1007/s00253-018-9050-1

Fardullah, M., Islam, M. S., Sarkar, M. S. U., Rahman, M. R., Akther, K., Hossain, M. T., & Robel, F. N. (2025). Heavy metal contamination and risk assessments in the surface water of Tanguar Haor, Bangladesh. *Geosystems and Geoenvironment*, *4*(3), Article 100399. https://doi.org/10.1016/j.geogeo.2025.100399

Freundlich, H. (1907). Über die Adsorption in Lösungen. *Zeitschrift für Physikalische Chemie*, *57*(1), 385-470. https://doi.org/10.1515/zpch-1907-5723

Fuge, R. (2013). Anthropogenic sources. In O. Selinus (Ed.). *Essentials of medical geology* (pp. 59-74). Springer. https://doi.org/10.1007/978-94-007-4375-5_4

Hansda, A., & Kumar, V. (2015). Biosorption of copper by bacterial adsorbents: A review. *Research Journal of Environmental Toxicology*, *9*(2), 45-58. https://doi.org/10.3923/rjet.2015.45.58

Ho, Y. S., & McKay, G. (1998a). A comparison of chemisorption kinetic models applied to pollutant removal on various sorbents. *Process Safety and Environmental Protection*, *76*(4), 332-340. https://doi.org/10.1205/095758298529696

Ho, Y. S., & McKay, G. (1998b). Sorption of dye from aqueous solution by peat. *Chemical Engineering Journal*, *70*(2), 115-124. https://doi.org/10.1016/S1385-8947(98)00076-X

Huang, W., & Liu, Z. M. (2013). Biosorption of Cd (II)/Pb (II) from aqueous solution by biosurfactant-producing bacteria: isotherm kinetic characteristic and mechanism studies. *Colloids and Surfaces B: Biointerfaces*, *105*, 113-119.

Jomova, K., Alomar, S. Y., Nepovimova, E., Kuca, K., & Valko, M. (2025). Heavy metals: Toxicity and human health effects. *Archives of Toxicology*, *99*(1), 153-209. https://doi.org/10.1007/s00204-024-03903-2

Karnwal, A. (2024). Unveiling the promise of biosorption for heavy-metal removal from water sources. *Desalination and Water Treatment*, *319*, Article 100523. https://doi.org/10.1016/j.dwt.2024.100523

Karabyn, V., & Kochmar, I. (2025). Distribution of different forms of manganese in coal mining waste: A case study of the Vizeyska mine, Ukraine. *IOP Conference Series: Earth and Environmental Science, 1499*(1), Article 012045. https://doi.org/10.1088/1755-1315/1499/1/012045

Karabyn, V., Shuryhin, V., Shutiak, S., Chmiel, M., & Kulhanek, R. (2022). Strategic environmental assessment – Underestimated tool for sustainable subsoil use. *Environmental Problems*, *7*(3), 140-146. https://doi.org/10.23939/ep2022.03.140

Khashei, S., Etemadifar, Z., & Rahmani, H. R. (2018). Immobilization of *Pseudomonas putida* PT in resistant matrices to environmental stresses: A strategy for continuous removal of heavy metals under extreme conditions. *Annals of Microbiology*, *68*(12), 931-942. https://doi.org/10.1007/s13213-018-1402-7

Kochmar, I., Karabyn, V., & Karabyn, O. (2022). Lead speciation in the technogenesis zone of coal mining sites (case of Vizeyska Mine of Chervonohrad Mining Area, Lviv Region, Ukraine). *Petroleum and Coal*, *64*(2), 445-454.

Kochmar, I., Karabyn, V., Stepova, K., Stadnik, V., & Sozanskyi, M. (2024). Thermal impact on heavy metal bioavailability in burnt rocks of waste heap of Chervonohradska coal-preparation plant (Lviv Region, Ukraine). *Geomatics and Environmental Engineering*, *18*(1), 117-133. https://doi.org/10.7494/geom.2024.18.1.117

Langmuir, I. (1918). The adsorption of gases on plane surfaces of glass, mica and platinum. *Journal of the American Chemical Society*, *40*(9), 1361-1403. https://doi.org/10.1021/ja02242a004

Lecca-Caballero, D., Vega-Moreno, E., Cabanillas-Chirinos, L., Del Aguila, K. D., Rojas-Villacorta, W., Salvatierra-Espinola, W., Naveda, R. N., Rojas-Flores, S., & De La Cruz-Noriega, M. (2023). An in vitro study of the effects of temperature and pH on lead bioremoval using *Serratia marcescens*. *Sustainability*, *15*(19), Article 14048. https://doi.org/10.3390/su151914048

Li, P.-S., & Tao, H.-C. (2015). Cell surface engineering of microorganisms towards adsorption of heavy metals. *Critical Reviews in Microbiology*, *41*(2), 140-149. https://doi.org/10.3109/1040841X.2013.813898

Li, X., Sun, M., Zhang, L., Finlay, R. D., Liu, R., & Lian, B. (2022). Widespread bacterial responses and their mechanism of bacterial metallogenic detoxification under high concentrations of heavy metals. *Ecotoxicology and Environmental Safety*, *246*, Article 114193. https://doi.org/10.1016/j.ecoenv.2022.114193

Loboichenko, V., Nikitina, N., Leonova, N., Konovalova, O., Bondarenko, A., Zemlianskyi, O., & Rashkevich, N. (2024). Study of the features of determination of heavy metals in bottom sediments. *IOP Conference Series: Earth and Environmental Science*, *1348*, Article 012014. https://doi.org/10.1088/1755-1315/1348/1/012014

Mahurpawar, M. (2015). Effects of heavy metals on human health. *International Journal of Research-Granthaalayah*, *3*(9SE), 1-7. https://doi.org/10.29121/granthaalayah.v3.i9se.2015.3282

Majhi, K., Let, M., Halder, U., & Bandopadhyayl, R. (2023). Copper adsorption potentiality of *Bacillus stercoris* GKSM6 and *Pseudomonas alcaliphila* GKSM11 isolated from Singhbhum copper mines. *Geomicrobiology Journal*, *40*(2), 193-202. https://doi.org/10.1080/01490451.2022.2137603

Masoumi, F., Khadivinia, E., Alidoust, L., Mansourinejad, Z., Shahryari, S., Safaei, M., Mousavi, A., Salmanian, A.-H., Zahiri, H. S., Vali, H., & Noghabi, K. A. (2016). Nickel and lead biosorption by *Curtobacterium* sp. FM01, an indigenous bacterium isolated from farmland soils of Northeast Iran. *Journal of Environmental Chemical Engineering*, *4*(1), 950-957. https://doi.org/10.1016/j.jece.2015.12.025

Martin, S., & Griswold, W. (2009). Human health effects of heavy metals. *Environmental Science and Technology Briefs for Citizens*, *15*, 1-6.

Mella, B., Glanert, A. C., & Gutterres, M. (2015). Removal of chromium from tanning wastewater and its reuse. *Process Safety and Environmental Protection*, *95*, 195-201. https://doi.org/10.1016/j.psep.2015.03.007

Meshram, S., Thakur, C., & Soni, A. B. (2020). Taguchi optimization of adsorptive treatment of effluent from lead-acid battery recycling unit using pressmud – a sugar industry waste. *Pollution*, *6*(4), 879-892.

Mitra, S., Chakraborty, A. J., Tareq, A. M., Emran, T. B., Nainu, F., Khusro, A., Idris, A. M., Khandaker, M. U., Osman, H., Alhumaydhi, F. A., & Simal-Gandara, J. (2022). Impact of heavy metals on the environment and human health: Novel therapeutic insights to counter the toxicity. *Journal of King Saud University – Science*, *34*(3), Article 101865. https://doi.org/10.1016/j.jksus.2022.101865

Mohapatra, R. K., Nayak, M., Parhi, P. K., Pandey, S., Thatoi, H., Panda, C. R., & Choi, Y. (2024). Biosorption performance and mechanism insights of live and dead biomass of halophilic *Bacillus altitudinis* strain CdRPSD103 for removal of Cd(II) from aqueous solution. *International Biodeterioration and Biodegradation*, *191*, Article 105811. https://doi.org/10.1016/j.ibiod.2024.105811

Mudgal, V., Madaan, N., Mudgal, A., Singh, R. B., & Mishra, S. (2010). Effect of toxic metals on human health. *The Open Nutraceuticals Journal*, *3*(1), 94-99. https://doi.org/10.2174/1876396001003010094

Naik, M. M., & Dubey, S. K. (2013). Lead resistant bacteria: Lead resistance mechanisms, their applications in lead bioremediation and biomonitoring. *Ecotoxicology and Environmental Safety*, *98*, 1-7. https://doi.org/10.1016/j.ecoenv.2013.09.039

Oladimeji, T. E., Oyedemi, M., Emetere, M. E., Agboola, O., Adeoye, J. B., & Odunlami, O. A. (2024). Review on the impact of heavy metals from industrial wastewater effluent and removal technologies. *Heliyon*, *10*(23), Article e40370. https://doi.org/10.1016/j.heliyon.2024.e40370

Othman, H. Q., & Hussein, Z. A. (2025). Assessment of radionuclide (radon, radium, and uranium) concentrations and heavy metal levels in blood samples from workers in concrete block factories. *Journal of Radiation Research and Applied Sciences*, *18*(1), Article 101306. https://doi.org/10.1016/j.jrras.2025.101306

Oyetibo, G. O., Ilori, M. O., Obayori, O. S., & Amund, O. O. (2014). Equilibrium studies of cadmium biosorption by presumed non-viable bacterial strains isolated from polluted sites. *International Biodeterioration and Biodegradation*, *91*, 37-44. https://doi.org/10.1016/j.ibiod.2014.03.004

Pejin, Đ., Pilipović, D. T., Tenodi, S., Veselić, D. R., Pautler, B. G., Sweett, A., & Krčmar, D. (2025). Integrated assessment of heavy metal pollution in the Great Bačka Canal: Comparing active and passive sampling methods. *Chemosphere*, *370*, Article 144027. https://doi.org/10.1016/j.chemosphere.2024.144027

Pereira, R. F. S., & de Carvalho, C. C. C. R. (2024). Improving bioprocess conditions for the production of prodigiosin using a marine *Serratia rubidaea* strain. *Marine Drugs*, *22*(4), Article 142. https://doi.org/10.3390/md22040142

Philip, L., Iyengar, L., & Venkobachar, C. (1998). Cr (VI) reduction by *Bacillus coagulans* isolated from contaminated soils. *Journal of Environmental Engineering*, *124*(12), 1165-1170. https://doi.org/10.1061/(ASCE)0733-9372(1998)124:12(1165)

Queiroz, P. S., Barboza, N. R., Cordeiro, M. M., Leão, V. A., & Guerra-Sá, R. (2018). Rich growth medium promotes an increased on Mn (II) removal and manganese oxide production by *Serratia marcescens* strains isolates from wastewater. *Biochemical Engineering Journal*, *140*, 148-156. https://doi.org/10.1016/j.bej.2018.09.018

Quiton, K. G., Doma, B. Jr, Futalan, C. M., & Wan, M.-W. (2018). Removal of chromium(VI) and zinc(II) from aqueous solution using kaolin-supported bacterial biofilms of Gram-negative *E. coli* and Gram-positive *Staphylococcus epidermidis*. *Sustainable Environment Research*, *28*(5), 206-213. https://doi.org/10.1016/j.serj.2018.04.002

Ren, G., Jin, Y., Zhang, C., Gu, H., & Qu, J. (2015). Characteristics of *Bacillus* sp. PZ-1 and its biosorption to Pb (II). *Ecotoxicology and Environmental Safety*, *117*, 141-148. https://doi.org/10.1016/j.ecoenv.2015.03.033

Rodríguez, C. E., Quesada, A., & Rodríguez, E. (2006). Nickel biosorption by *Acinetobacter baumannii* and *Pseudomonas aeruginosa* isolated from industrial wastewater. *Brazilian Journal of Microbiology*, *37*(4), 465-467. https://doi.org/10.1590/S1517-83822006000400012

Sharafi, S. & Salehi, F. (2025). Comprehensive assessment of heavy metal (HMs) contamination and associated health risks in agricultural soils and groundwater proximal to industrial sites. *Scientific Reports*, *15*(1), Article 7518. https://doi.org/10.1038/s41598-025-91453-7

Sutherland, C. (2004). *Removal of heavy metals from waters using low-cost adsorbents: Process development* [Doctoral dissertation, The University of the West Indies, St. Augustine]. UWI Institutional Repository. https://hdl.handle.net/2139/3777

Sutherland, C. (2024). Adsorption of cephalexin: A decade of progress in adsorbent development and mechanistic insights. *Desalination and Water Treatment*, *318*, Article 100357. https://doi.org/10.1016/j.dwt.2024.100357

Sutherland, C. (2025). A method of classifying the influence of intraparticle diffusion in adsorption systems: characteristic curves of the diffusion-chemisorption kinetic

model. *Environmental Toxicology and Chemistry*, *44*(5), 1209-1221. https://doi.org/10.1093/etojnl/vgaf052

Sutherland, C., Chittoo, B. S., Venkobachar, C. (2017). Application of an artificial neural network–genetic algorithm methodology for modelling and optimization of the improved biosorption of a chemically modified peat moss: Kinetic studies. *Desalination and Water Treatment*, *84*, 69-84. https://doi.org/10.5004/dwt.2017.21197

Sutherland, C., Chittoo, B. S., & Samlal, A. (2023). The status of scientific development on the application of biosorption of heavy metals at laboratory and pilot-scale: a review. *Desalination and Water Treatment*, *299*, 13-49. https://doi.org/10.5004/dwt.2023.29699

Sutherland, C., & Venkobachar, C. (2010). A diffusion–chemisorption kinetic model for simulating biosorption using forest macro-fungus, *Fomes fasciatus*. *International Research Journal of Plant Science*, *1*(4), 107-117.

Sutherland, C., & Venkobachar, C. (2020). Regeneration of a chemically improved peat moss for the removal and recovery of Cu(II) and Pb(II) from aqueous solution. *Desalination and Water Treatment*, *178*, 172-181. https://doi.org/10.5004/dwt.2020.24945

US EPA. (2008). *Fate, transport, and transformation test guidelines,* OPPTS 835.1230 *adsorption/desorption (batch equation)*. U.S. Environmental Protection Agency.

Truskewycz, A., Gundry, T. D., Khudur, L. S., Kolobaric, A., Taha, M., Aburto-Medina, A., Ball, A. S., & Shahsavari, E. (2019). Petroleum hydrocarbon contamination in terrestrial ecosystems—fate and microbial responses. *Molecules*, *24*(18), Article 3400. https://doi.org/10.3390/molecules24183400

Veglio, F., & Beolchini, F. (1997). Removal of metals by biosorption: A review. *Hydrometallurgy*, *44*(3), 301-316. https://doi.org/10.1016/S0304-386X(96)00059-X

Weber, W. J. Jr., & Morris, J. C. (1963). Kinetics of adsorption on carbon from solution. *Journal of the Sanitary Engineering Division*, *89*(2), 31-59. https://doi.org/10.1061/JSEDAI.0000430

Wolf, A., Bunzl, K., Dietl, F., & Schmidt, W. F. (1977). Effect of Ca^{2+} ions on the absorption of Pb^{2+}, Cu^{2+}, Cd^{2+} and Zn^{2+} by humic substances. *Chemosphere*, *6*(5), 207-213. https://doi.org/10.1016/0045-6535(77)90003-0

Wu, F.-C., Tseng, R.-L., & Juang, R.-S. (2009). Initial behavior of intraparticle diffusion model used in the description of adsorption kinetics. *Chemical Engineering Journal*, *153*(1-3), 1-8. https://doi.org/10.1016/j.cej.2009.04.042

Xing, R., Li, Y., Zhang, B., Li, H., & Liao, X. (2017). Indicative and complementary effects of human biological indicators for heavy metal exposure assessment. *Environmental Geochemistry and Health*, *39*(5), 1031-1043. https://doi.org/10.1007/s10653-016-9870-9

Zahra, N., Kalim, I., Mahmood, M., & Naeem, N. (2017). Perilous effects of heavy metals contamination on human health. *Pakistan Journal of Analytical and Environmental Chemistry*, *18*(1), 1-17. https://doi.org/10.21743/pjaec/2017.06.01

Zakeri, F., Noghabi, K. A., Sadeghizadeh, M., Kardan, M. R., Masoomi, F., Farshidpour, M. R., & Atarilar, A. (2010). *Serratia* sp. ZF03: An efficient radium biosorbent isolated from hot-spring waters in high background radiation areas. *Bioresource Technology*, *101*(23), 9163-9170. https://doi.org/10.1016/j.biortech.2010.07.032